COGNITIVE NEUROSCIENCE

Brain connectivity–based prediction of real-life creativity is mediated by semantic memory structure

Marcela Ovando-Tellez[1]*, Yoed N. Kenett[2], Mathias Benedek[3], Matthieu Bernard[1], Joan Belo[1], Benoit Beranger[4], Theophile Bieth[1,5], Emmanuelle Volle[1]*

Associative theories of creativity argue that creative cognition involves the abilities to generate remote associations and make useful connections between unrelated concepts in one's semantic memory. Yet, whether and how real-life creative behavior relies on semantic memory structure and its neural substrates remains unclear. We acquired multi-echo functional magnetic resonance imaging data while participants underwent a semantic relatedness judgment task. These ratings were used to estimate their individual semantic memory networks, whose properties significantly predicted their real-life creativity. Using a connectome predictive modeling approach, we identified patterns of task-based functional connectivity that predicted creativity-related semantic memory network properties. Furthermore, these properties mediated the relationship between functional connectivity and real-life creativity. These results provide new insights into how brain connectivity patterns support real-life creative behavior via the structure of semantic memory. We also show how computational network science can be used to couple behavioral, cognitive, and neural levels of analysis.

INTRODUCTION

Creativity is key to our ability to cope with change, innovate, and find new solutions to address societal challenges. Understanding the complex and multidimensional construct of creativity is thus fundamental to support societal, cultural, and economic progress. Creative behavior in real life depends on individual differences in cognitive ability, in addition to personality and environmental factors (*1*). The cognitive mechanisms underlying creative abilities are not yet fully understood, but pertinent theories of creative cognition consistently highlight the role of specific associative processes and the need to uncover meaningful links between unrelated concepts (*2–7*).

The associative theory of creative thinking hypothesizes that creative abilities are related to the organization of associations in semantic memory (*6*). In support of the associative theory, several studies found that more creative individuals are able to more easily link distant concepts: They provide lower estimates of the remoteness of unrelated words than less creative individuals (*8*), are faster in judging the relatedness of concepts (*9*), have less common or constrained word associations in free generation tasks (*3, 10, 11*), and have a more flexible organization of semantic memory (*2, 7, 12–14*). Other studies have specifically demonstrated the important role of dissociation ability and associative combination in creative thinking (*2–4, 15, 16*). In addition, in brain-damaged patients, rigid semantic associations were associated with poor creative abilities (*17, 18*). Associative thinking has been related to creative abilities as measured within several existing frameworks, such as divergent thinking (*2–4, 8, 19*), insight problem solving (*6*), and analogical reasoning (*20*), as well as to creative achievements in real life (*11, 15, 21*). For instance, creative behavior in real life has been related to associative

processes including generating remote semantic associations (*11*) or bi-associations (*15*). Overall, there is ample evidence that the way in which concepts are associated and activated via associative processes relies on the structure of semantic memory, which influences the ability to connect remote concepts into novel ideas (*5, 7, 22–24*), and, thereby, semantic memory has a critical role in creativity.

Recent research has demonstrated how computational network science methodologies (*25*) based on mathematical graph theory allow exploring the structure of semantic memory via semantic networks (SemNets). Applying these methods, several studies have shown that creative abilities can be related to the structure of semantic memory (*5, 13, 14, 23, 24, 26*). Kenett *et al.* (*14*) investigated the SemNets of groups of low and high creativity individuals on the basis of free associations generated by both groups to a list of 96 cue words. They found that the SemNets of low creativity individuals were less connected and more spread out compared to the SemNets of high creativity individuals. However, estimating SemNets at the group level may obscure individual differences related to creativity. To address this issue, Benedek *et al.* (*13*) developed a method to estimate individual SemNets on the basis of word relatedness judgment ratings. Participants made relatedness judgments on the relationship between all possible pairs of 28 cue words, serving as a proxy for the organization of these words in an individual's semantic memory. They demonstrated how individual-based SemNet metrics replicated the group-based findings of Kenett *et al.* (*14*) and were related to individual differences in divergent thinking scores [the most widely assessed component of creative thinking (*27*)]. The findings of Benedek *et al.* (*13*) have since been replicated across different languages (*5, 26, 28*), demonstrating the validity of this approach.

In a previous study (*26*), we replicated and extended the approach developed by Benedek *et al.* (*13*) with two improvements: We controlled the selection of the cue words using a computational method optimizing the distribution of theoretical distances between words, and we assessed creative abilities and behaviors using a more diverse set of tools. Our previous study showed that the network metrics of individual SemNets, built from the relatedness judgments the participants gave to several pairs of words, correlated with several

[1]Sorbonne University, FrontLab at Paris Brain Institute (ICM), INSERM, CNRS, 75013 Paris, France. [2]Faculty of Industrial Engineering and Management, Technion–Israel Institute of Technology, Haifa 3200003, Israel. [3]Institute of Psychology, University of Graz, Graz, Austria. [4]Sorbonne University, CENIR at Paris Brain Institute (ICM), INSERM, CNRS, 75013 Paris, France. [5]Neurology Department, Pitié-Salpêtrière Hospital, AP-HP, F-75013 Paris, France.
*Corresponding author. Email: emmavolle@gmail.com (E.V.); marcela.ovandot@gmail.com (M.O.-T.)

measures of creativity, including a questionnaire of creative activities and achievements (29). Hence, individual SemNet measures allow exploring the underlying cognitive mechanisms of creativity by revealing how different aspects of the semantic memory structure relate to creativity and to creative behavior (5). However, the neurocognitive determinants of individual differences in creativity related to the structure of semantic memory are still unclear and unexplored.

Existing magnetic resonance imaging (MRI)–based neuroimaging studies have identified a large set of brain regions involved in creative cognition (7, 30–32). A growing body of creativity neuroscience research has highlighted the importance of functional interactions within and between several brain networks, including the executive control network, the salience network, and the default mode network (30). In addition, semantic and episodic memory regions (32–35) and the motor and premotor regions have been shown to play a role in creative cognition (32, 36). Evidence from studies in semantic cognition has further linked creativity to neural interactions between semantic representations and control processes (37). These components of semantic cognition draw on different brain regions (38), with anterior temporal lobes (partially overlapping with default mode network) critical for heteromodal conceptual information in long-term memory and regions interspersed between default mode network and multiple-demand network supporting semantic control (39, 40). The advantage of a whole-brain functional connectivity approach is to provide a holistic and functional view of how brain networks relate to creative thinking. For example, resting-state functional connectivity within and between these networks was shown to predict creative abilities (31), and task-based functional connectivity within and between these networks increased during a creativity task, compared to a control task (30, 31). A recent approach in neuroimaging research is connectome predictive modeling (CPM) (41), which uses machine learning methods to identify patterns of functional connectivity that predict complex cognitive functions, including divergent thinking ability (31, 41, 42). Unlike previous research that focused on the brain connectivity associated with specific creativity tasks (e.g., divergent thinking), the current study explores the neurocognitive determinants of real-life creativity by studying the neural basis of semantic memory organization related to creative behavior. We hypothesized that the associative mechanisms reflected by SemNet metrics are relevant to real-life creative activities and achievements and can be predicted by functional connectivity patterns, involving, in particular, the control, default, and salience networks (31).

To this end, we first examine the properties of individual SemNets via network metrics and identify SemNet metrics that reliably predict differences in creative achievement and activities and thus constitute cognitive markers of real-life creativity. We then explore the functional connectivity of brain networks predicting individual differences in these SemNet markers. We use the CPM method and analyze functional brain connectivity during the performance of the semantic relatedness task that is used to estimate individual SemNets. This allows us to identify the task-based functional connectivity patterns predicting individual differences in SemNet properties. As an internal validation, we additionally explore whether the predictive models built in the task-based functional connectivity are generalizable to participants' resting-state functional connectivity. Last, we examine whether SemNet properties mediate the link between these brain connectivity patterns and real-life creativity, thus linking functional connectivity to real-life creativity via individual differences in semantic memory organization.

RESULTS

Individual SemNet metrics and creativity

First, we explored the properties of individuals' SemNets in relation to creativity. Similar to previous studies (5, 13, 26), we estimated participants' individual semantic memory network as weighted (WUN) and unweighted (UUN) undirected networks based on performance in the semantic relatedness judgment task (RJT; Fig. 1). During the RJT, participants judged the relatedness between all possible pairs of 35 words (595 ratings).

In undirected networks, the relation between node a and node b is equal to the relation between node b and node a, which conforms to the nature of the judgment task. WUN and UUN differ in either assuming weighted or unweighted network links. The WUN is a more informed type of SemNet as it retains the weights of all links between the words (nodes). The UUN is a binary network that only retains the links between words (nodes) that are moderately or highly associated (i.e., ratings greater than 50 on the visual scale; Fig. 1A) and sets their weights to 1. We built these two types of networks, UUN and WUN, as previous studies had suggested that they are particularly sensitive to creative ability (5, 13, 26), with subtle differences across creativity measures (5, 13, 26). Therefore, we aimed to explore whether the properties of a more informed (WUN) or less informed (UUN) network are better captured by the individual's brain functional connectivity patterns during the RJT task. We then computed established network measures in cognitive network research (25) for WUN and UUN that have been previously related to creative abilities (5, 13, 14, 24, 26) including the following: average shortest path length (ASPL; measuring average distances or the spread of the SemNet), clustering coefficient (CC; measuring overall connectivity in the SemNet), modularity (Q; measuring the level of segregation of the SemNet), and small worldness (S; measuring the ratio between connectivity and distances in the network; see Materials and Methods). In addition, we assessed individual differences in real-life creative activities (C-Act) and achievements (C-Ach) via the Inventory of Creative Activities and Achievements (ICAA; see also section S3) (29) completed outside the MRI scanner (descriptive statistics for behavioral and network measures are reported in Table 1). On the basis of previous studies that related SemNets to creative abilities (5, 13, 14, 24, 26), we expected higher creative behavior (higher C-Act and/or C-Ach scores) to be related to more connected and flexible (higher CC and S), less spread out (lower ASPL), or less segregated (lower Q) networks. Given that most previous work had focused on creative potential, we had no strong expectation on differences between predictions regarding WUN and UUN in the context of creative behavior.

We then examined how SemNet metrics predict real-life creativity by applying linear regression models, regressing creativity on each SemNet metric with leave-one-out cross-validations: We iteratively fitted predictive linear models in $N - 1$ participants and tested the model in the left-out participant. The significance of the model prediction was assessed by the correlation between the predicted value of C-Act (or C-Ach) computed by the model and the observed value using permutation testing. These analyses revealed that both real-life creative activities and achievements are predicted from different individual SemNet metrics (Fig. 2). The Spearman correlations showing the direction and size of the relationships between SemNet metrics and creativity are reported in Table 2. C-Act was predicted from WUN ASPL and UUN Q. C-Ach was predicted from WUN Q and UUN Q. Overall, more creative individuals had less modular SemNets. To ensure that the results were not affected by age, sex, education,
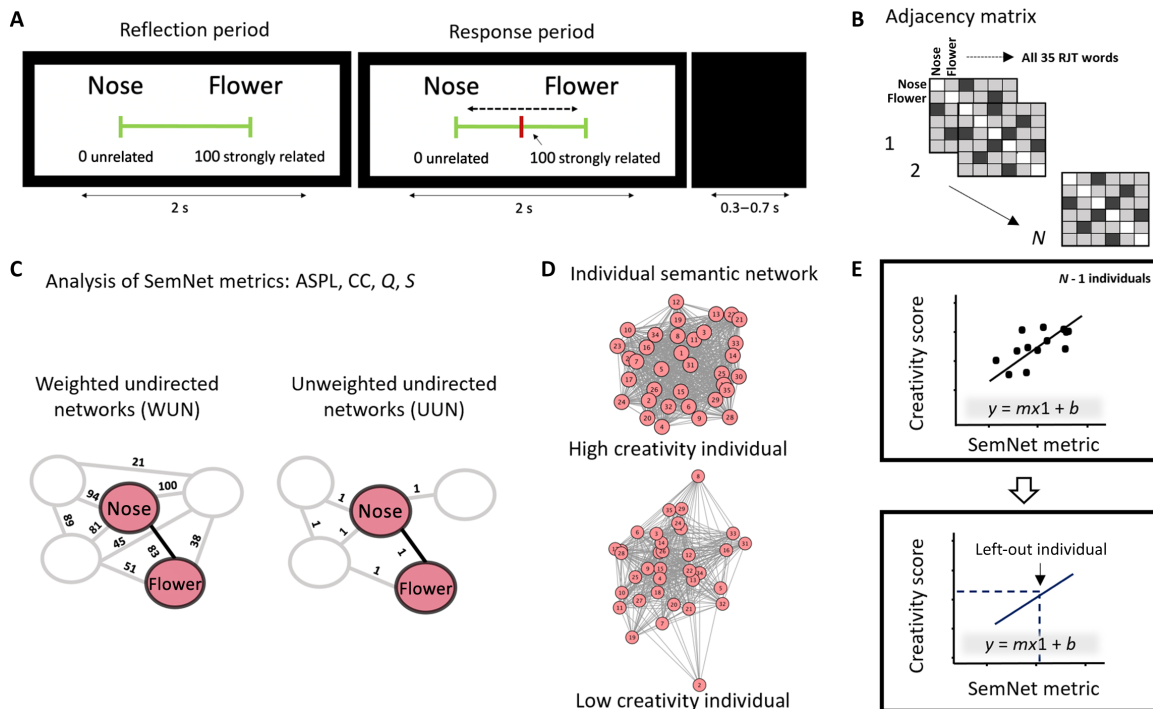
Fig. 1. Estimation of individual SemNets to predict creativity. (**A**) Trial representation of an exemplary trial of the RJT asking participants to judge the relatedness of 595 word pairs. Each trial began with the display of a pair of words along with a visual scale (reflection period) ranging from 0 (unrelated words) to 100 (strongly related words). During the next 2 s (response period), participants were allowed to move the cursor (in red) using a trackball to indicate the relatedness of the two words. An intertrial interval of 0.3- to 0.7-s separated trials. (**B**) For each participant, we computed a 35 by 35 adjacency (connectivity) matrix with columns and rows representing each of the 35 RJT words, and cell values corresponding to the relatedness judgments given by the participant during the RJT. (**C**) We estimated individual semantic memory networks following two established approaches: WUN and UUN, using the RJT words as the network nodes. In the WUN, the RJT judgments reflected the strength of links between nodes. In the UUN, the RJT judgments above average (50) were kept and set to one. The SemNet metrics were computed for both WUN and UUN separately: ASPL, CC, Q, and S. (**D**) Representation of the individual WUN SemNets for a low creativity participant and a high creativity participant. (**E**) Linear regressions using leave-one-out cross-validations were performed to explore whether real-life creative activities (C-Act) and achievements (C-Ach) were predicted from SemNet properties estimated in (B). The SemNet metrics were used to build predictive linear models in $N - 1$ participants. The predictive model was tested on the left-out participant using its SemNet metric (m) to predict its creativity scores. ASPL, average shortest path length; CC, clustering coefficient; Q, modularity; S, small worldness.

and intelligence quotient (IQ), we explored the correlations between these variables and SemNet metrics and creativity scores (table S1). The results remained significant after controlling for the variables that correlated with either the SemNet metrics or the creativity scores (fig. S1).

Prediction of creativity-related SemNet properties from brain connectivity

We applied the CPM approach (31, 41) to explore whether task-based functional connectivity patterns predict semantic memory network metrics that related to creativity (i.e., Q in WUN and UUN and ASPL in WUN; see Table 2; the applied CPM approach is illustrated in Fig. 3). We used a functional brain atlas to define 200 brain nodes belonging to 17 functional networks (43). For each participant, Pearson correlations of the blood oxygen level–dependent (BOLD) signal between all unique pairs of brain regions (i.e., nodes; $n = 19,900$) were computed to estimate the task-related functional connectivity of the whole-brain connectivity network (Fig. 3A). We then identified relevant links of the brain connectivity network that positively (positive model network) or negatively (negative model network) correlated with the SemNet metric across participants (Fig. 3B). Next, we adapted the classical CPM method (41) to better take into account the network properties of the brain model networks. Instead

of using the sum of the connectivity in the model networks, we computed two key network metrics describing small-worldness properties of human brain networks (44, 45): their CC (brain-CC) and efficiency (brain-Eff) (Fig. 3C). We selected these brain network metrics because the small-world organization of the brain networks has been widely supported in network neuroscience (44). Such research has characterized the brain by a high clustering (brain-CC) and long-distance connection, allowing efficient local and global information processing and integration (brain-Eff; measured as the inverse of the ASPL). Long-distance connections (as measured by brain-Eff) were shown to support the functional diversity of the whole brain acting as an integrated brain network (46). In addition, brain-Eff has been previously correlated to personality traits related to creative behaviors (47). We then ran six separate linear models regressing each SemNet metric (Q for WUN and UUN and ASPL for WUN) on each model network metric (brain-CC and brain-Eff). We used leave-one-out cross-validations, iteratively fitting predictive linear models in $N - 1$ participants and tested these models on the left-out participant (Fig. 3D). Last, the model prediction was assessed by the Spearman correlation between the predicted value from the model and the observed values.

We then tested the relation between predicted and observed CPM models on the various SemNet metrics, using 1000 iteration

Table 1. Descriptive statistics of creativity scores and SemNet measures. Data are shown for real-life creativity activities (C-Act) and achievements (C-Ach) and for SemNet metrics of weighted (WUN) and unweighted (UUN) networks. ASPL, average shortest path length; CC, clustering coefficient; Q, modularity; S, small worldness.

|	Means	SD	Min	Max	Skewness	Kurtosis
Creativity scores						
C-Act	47.894	21.695	13	102	0.428	−0.609
C-Ach	74.638	42.249	1	207	0.744	0.507
WUN metrics						
ASPL	0.021	0.004	0.015	0.037	1.713	3.353
CC	0.363	0.096	0.142	0.628	0.274	0.267
Q	0.122	0.058	0.032	0.319	1.037	1.436
S	1.003	0.073	0.828	1.387	1.913	9.134
UUN metrics						
ASPL	1.633	0.221	1.262	2.361	1.456	2.665
CC	0.585	0.082	0.438	0.781	0.130	−0.658
Q	0.178	0.064	0.058	0.392	0.919	1.387
S	1.386	0.271	1.011	2.936	2.628	11.269
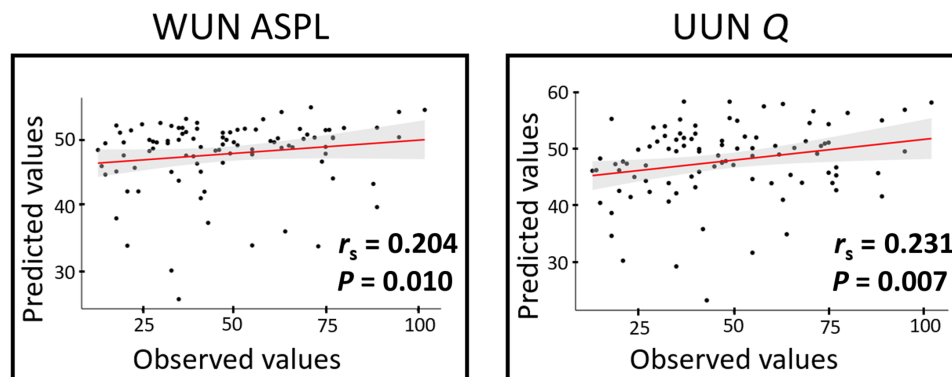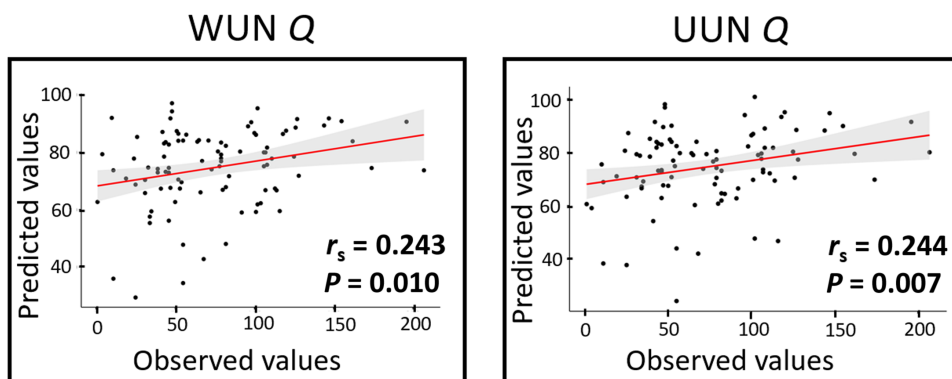
Fig. 2. Prediction of creativity scores from SemNet metrics. The plots show the Spearman correlations between the predicted values (y axis) and observed values (x axis) of creative activities and achievements based on individual SemNet metrics for the significant predictions. At the bottom-right part of each plot, we present the r_s and the P values, based on permutation testing.

Table 2. Relationship between individual SemNet metrics and creativity. The Spearman correlations between SemNet metrics and creativity scores are reported (r_s for C-Act and C-Ach). In bold are the significant predictions of creativity from the SemNet properties after permutation testing shown in Fig. 2.

Creativity scores	C-Act		C-Ach	
	r_s	P	r_s	P
WUN metrics				
ASPL	**−0.276**	**0.007***	−0.208	0.044
CC	0.165	0.111	0.201	0.052
Q	−0.179	0.085	**−0.295**	**0.004***
S	0.234	0.023	−0.017	0.868
UUN metrics				
ASPL	−0.125	0.230	−0.149	0.152
CC	0.092	0.378	0.080	0.441
Q	**−0.281**	**0.006***	**−0.287**	**0.005***
S	−0.154	0.139	−0.219	0.034

*Correlations that reached significance after false discovery rate correction for multiple comparisons.

permutation testing (Fig. 4) (*41*). The CPM-based prediction from brain-CC was significant for the WUN Q metric ($r_s = 0.386$, $P = 0.004$). The CPM-based predictions from brain-Eff were significant for the WUN Q metric ($r_s = 0.476$, $P = 0.001$) and the UUN Q metric ($r_s = 0.272$, $P = 0.036$). The CPM-based predictions of WUN ASPL from both brain-CC and brain-Eff and UUN Q from brain-CC were not significant, showing either a negative correlation between predicted and observed values (indicating the prediction model failure) or not significant P value after permutation testing. These results remained significant after controlling for variables (fig. S2) that correlated with either the SemNet metrics or ICAA scores (table S1), i.e., sex, education, and IQ, suggesting that our findings are robust to individual differences in these factors. In summary, CPM analyses on task-based functional connectivity showed that brain connectivity CC and efficiency allowed reliable predictions of SemNet Q.

Functional anatomy of the predictive brain connectivity patterns

To characterize the functional brain connectivity patterns predictive of SemNet metrics, we explored the links of the model networks that account for SemNet properties relevant to creativity. Unique positive and negative model networks were identified for each SemNet metric (Fig. 3B) (*41*) and were used to compute their network properties (brain-CC and brain-Eff; Fig. 3C). Because SemNet modularity (Q) was negatively correlated with both creativity measures (C-Act and
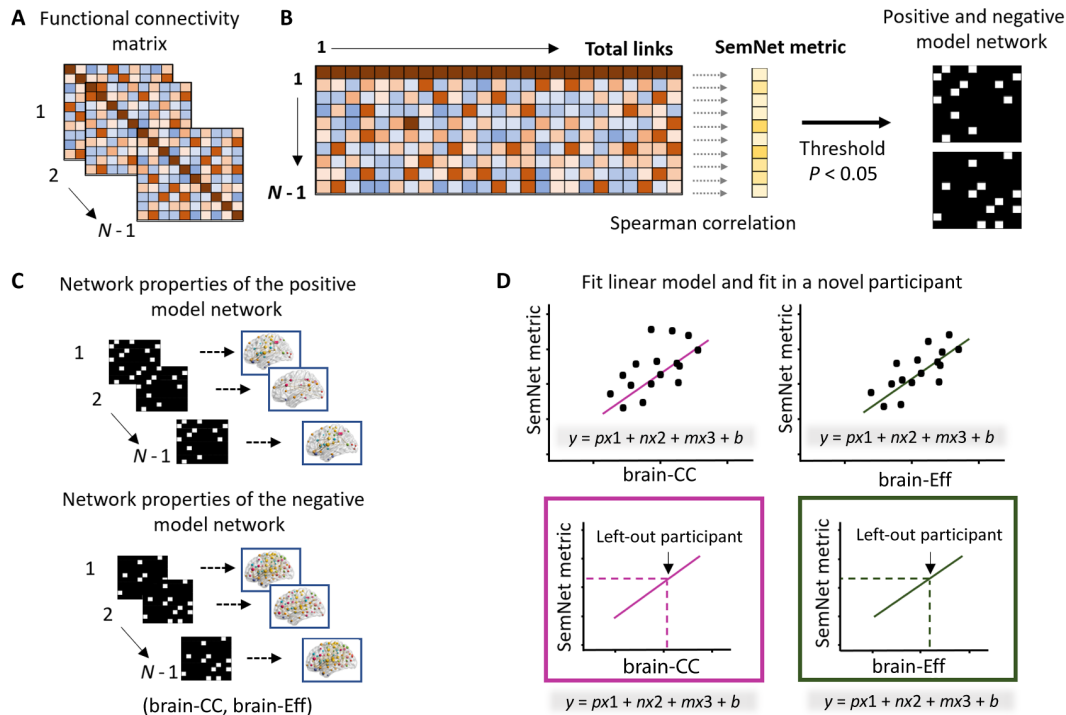

Fig. 3. CPM-based prediction method. (**A**) We defined the brain nodes on the basis of the Schaefer atlas consisting of 200 regions of interests (ROIs) (*43*). For each participant, we assessed the BOLD activity during the RJT in each ROI and used pairwise Pearson correlations to estimate a 200 by 200 task-related functional connectivity matrix. Using a leave-one-out approach, all the CPM steps were conducted in N − 1 participants. (**B**) The functional connectivity matrix (all links) was correlated to SemNet metrics using Spearman correlations. The links that significantly positively or negatively correlated with the SemNet metric (P < 0.05) formed a positive and a negative model network, respectively. (**C**) We calculated two network properties (in separate CPM analyses) of the positive and negative model networks, brain-CC and brain-Eff metrics. (**D**) The brain metrics in the positive (*p*) and negative (*n*) model networks were used to build a linear model predicting the SemNet metric in the left-out participant. Because head motion can affect CPM, we included the mean FD variable (*m*), a head motion parameter, as a regressor in the model to avoid a possible effect in the prediction. Last, the model was applied to the left-out participant to compute a predicted SemNet value from his/her brain model networks. The predicted value was then correlated with the observed value to assess the model predictive validity.
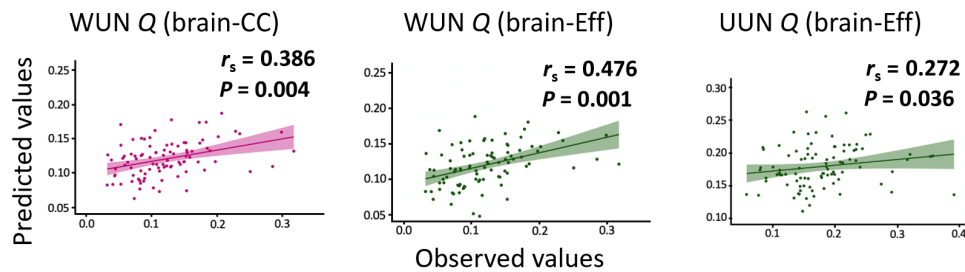
Fig. 4. Predicted and observed SemNet metrics. The plots show the Spearman correlations between the predicted values (*y* axis) and observed values (*x* axis) of SemNet metrics based on brain connectivity for the significant predictions. Green plots are presented for brain-Eff and magenta ones for brain-CC. In the upper-right side of each plot, we present the r_s and the *P* values. The reported *P* values are based on permutation testing.

C-Ach; Table 2), as expected from previous studies (*5, 13, 14, 26*), we focused on the description of the negative model network predicting UUN *Q* (Fig. 5) or WUN *Q* (fig. S3). In this model network, we considered the links that were shared in all iterations of the leave-one-out analysis, as the links in the model network can slightly vary at each iteration.

For the standard CPM-negative model network of UUN *Q*, we identified 452 links. The connectivity of these links was related to lower SemNet *Q*, which again predicted higher real-life creativity. These links represented connections mainly within and between temporal, parietal, limbic, and prefrontal lobes (Fig. 5, A and B). When we explored the distribution of these links at the functional networks level, on the basis of the functional networks included in the Schaefer atlas (*43*), most of the links were part of the somatomotor, salience, and default mode networks (Fig. 5C). The highest number of links were found between control and default mode networks (8.2%), followed by links within the salience network and between somatomotor and visual networks. In this model network, the highest-degree nodes, nodes with the highest number of connections (*k*; i.e., the number of functional connections), belonged to the right hemisphere being part of the visual network (i.e., extrastriate inferior, *k* = 53), default mode network (i.e., medial prefrontal cortex, *k* = 39), salience (i.e., insula, *k* = 31; parietal medial, *k* = 28), temporoparietal (i.e., temporal-parietal; *k* = 29), and limbic (temporal pole, *k* = 28) networks (Fig. 5D). In summary, the main patterns of functional connectivity that predicted lower SemNet *Q* (i.e., related to higher creativity) had a whole-brain distribution and involved the control, default mode, salience, and somatomotor networks.

Internal validation: Prediction of creativity-related SemNet properties from resting-state functional connectivity

We then explored whether the predictive models built on the basis of the task-based functional connectivity data can be generalized to the prediction of SemNet metrics from the resting-state functional connectivity. To this end, we used the positive- and the negative-network models from the task-based functional connectivity data from all participants to build the predictive model for UUN *Q* and WUN *Q* (using the same method as for the task-based functional connectivity prediction described above but with all participants included). We then applied these predictive models to the participants' resting-state data by computing the brain-Eff and brain-CC of the model networks during resting state for each participant. The model prediction was assessed by the Spearman correlation between the predicted value from the model and the observed values. The CPM-based prediction from brain-CC of resting-state connectivity

was significant for the WUN *Q* metric (r_s = 0.210, *P* = 0.043). The CPM-based predictions from brain-Eff of resting-state connectivity was significant for the WUN *Q* metric (r_s = 0.267, *P* = 0.010) but not for the UUN *Q* metric (r_s = 0.103, *P* = 0.327) (Fig. 6). Thus, the predictive model of creativity-related SemNet properties built on task-based functional connectivity data was also partly significant when applied to the brain intrinsic connectivity data of the individuals. This result suggests that properties of memory structure, and particularly the modularity metric, are also represented in intrinsic functional connectivity. Critically, this result support the CPM-based predictive model's robustness and generalization to the resting-state functional MRI (fMRI) data (*31*).

Mediation analysis

In the previous analyses, we found a relationship between SemNets and real-life creativity and between brain functional connectivity and SemNets. In a final step, we analyzed whether the relationship between task-based functional brain connectivity and real-life creativity is mediated by the SemNet properties. Hence, we conducted mediation analyses that focused on the indirect effect of functional connectivity on creative activities and achievements, using either C-Act or C-Ach as the dependent variable for each significant CPM model. To simplify interpretations, because UUN *Q* had a negative correlation with creativity, its value was reversed (UUN Q_R) to be positively correlated with creativity. Hence, lower modularity of the SemNet can be described as a higher flexibility of the SemNet (*23, 24, 48*).

Because C-Act was significantly predicted by the SemNet metric UUN *Q*, we explored the mediating role of UUN *Q* on the relationship between the properties of the functional brain network predicting UUN *Q* (brain-Eff) and C-Act (Fig. 7A). As shown in the previous analyses, the regression coefficient between brain-Eff and UUN Q_R was statistically significant (beta = 0.305, *P* < 0.001), as was the regression coefficient between UUN Q_R and C-Act (beta = 0.443, *P* = 0.002). The total effect and the direct effect were not statistically significant (beta = 0.116, *P* = 0.328; beta = −0.019, *P* = 0.872). In all mediation analyses, we calculated the indirect effect as the product of path a (i.e., the regression coefficient between brain functional connectivity and SemNet metric) and path b (i.e., the regression coefficient between SemNet metric and creativity) (Fig. 7). We tested the significance of the indirect effect using a bootstrapping method. The bootstrapped indirect effect was (0.305) × (0.443) = 0.135, and the 95% confidence interval ranged from 0.024 to 0.320. Thus, the indirect effect was statistically significant (*P* = 0.002). Hence, SemNets UUN *Q* mediated the relationship between the efficiency of functional brain connectivity (brain-Eff) and creative activities (C-Act):
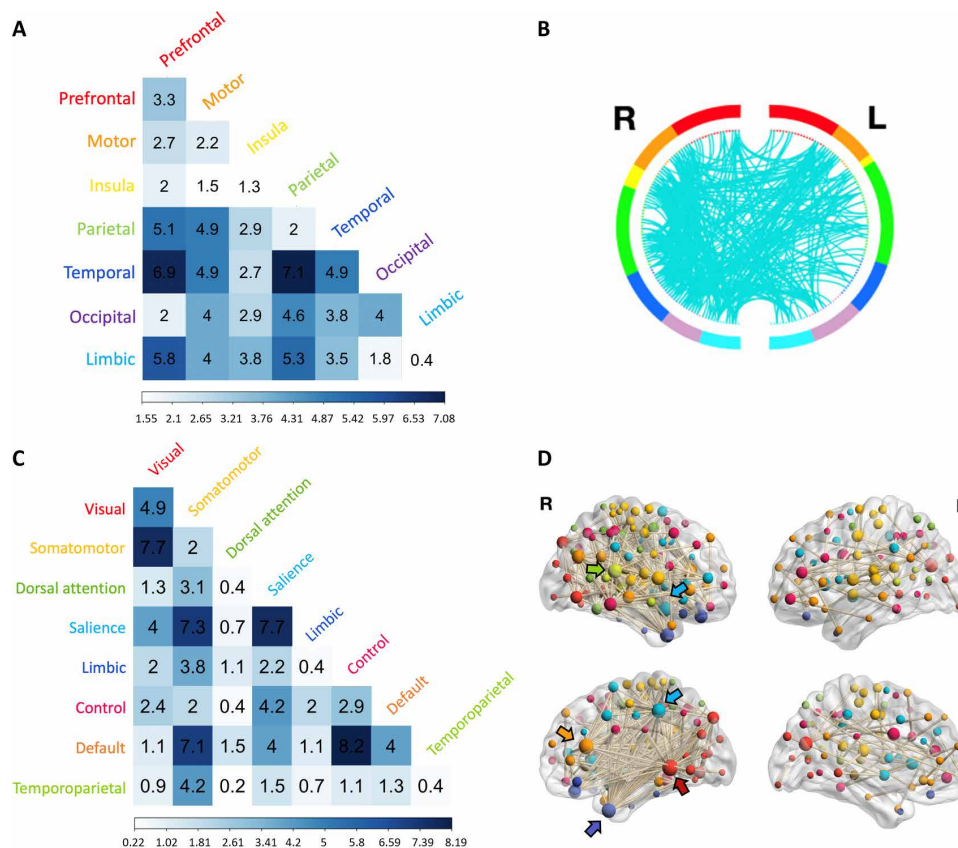
Fig. 5. Functional anatomy of the CPM model predicting the SemNet metric UUN Q. (A) First, we examined the distribution of the links of the model network at the brain location level, specifically into the brain lobes. The correlation matrix represents the percentage of links within the model network connecting seven different brain lobes (total links = 452). (**B**) A circular graph represents the distribution of links within and between brain regions in the left (L) and right (R) hemispheres. Brain regions are color-coded as in (A), and the cyan lines represent the links connecting the ROIs. For visualization purposes, we used a nodal degree threshold of $k > 10$. (**C**) Second, we examined the distribution of the links across intrinsic functional networks on the basis of Schaefer's atlas (*43*). The matrix represents the percentage of links within the model network (i.e., within the 452 links) occurring within and between eight intrinsic brain networks. (**D**) The nodes and links of the model network are superimposed on a volume rendering of the brain. The color of the nodes represents the functional network they belong to, using a similar color code as in (B). The size of the nodes is proportional to their degree, and the highest-degree nodes are marked by arrows. Nodes with degree $k = 0$ are not displayed.

The higher the efficiency of the negative model network that predicts UUN Q, the lower the SemNet Q, and the higher are real-life creative activities.

C-Ach score was predicted from SemNet WUN Q and UUN Q metrics. We explored the mediating role of UUN Q between the functional connectivity of the negative model network predicting it (brain-Eff) and C-Ach (Fig. 7B). The mediation analysis showed that the regression coefficient between brain-Eff and UUN Q_R was statistically significant (beta = 0.305, $P < 0.001$), as was the regression coefficient between the C-Ach and UUN Q_R (beta = 0.241, $P = 0.005$). The total effect and the direct effect were not statistically significant (beta = 0.142, $P = 0.056$; beta = 0.069, $P = 0.353$). The bootstrapped indirect effect was $(0.305) \times (0.241) = 0.073$, and the 95% confidence interval ranged from 0.018 to 0.140. Thus, the indirect effect was statistically significant ($P < 0.001$). Hence, SemNets UUN Q mediated the link between the efficiency of brain functional connectivity (brain-Eff) and real-life creative achievements (C-Ach): The higher the efficiency of the negative model network that predicts UUN Q, the lower the modularity of SemNet, and the higher the real-life creative achievements.

Similarly, we explored the mediating role of WUN Q on the relationship between the properties of the functional connectivity of the negative model network predicting it (brain-Eff and brain-CC) and C-Ach (Fig. 7C). Using brain-Eff as an independent variable, the regression coefficient between brain-Eff and WUN Q_R was significant (beta = 0.286, $P = 0.004$), as was the regression coefficient between C-Ach and WUN Q_R (beta = 0.183, $P = 0.015$). The total effect and the direct effect were not statistically significant (beta = 0.094, $P = 0.183$; beta = 0.042, $P = 0.560$). The bootstrapped indirect effect was $(0.286) \times (0.183) = 0.052$, and the 95% confidence interval ranged from 0.005 to 0.110. Thus, the indirect effect was statistically significant ($P = 0.018$).

Using brain-CC as an independent variable, the regression coefficient between brain-CC and WUN Q_R was significant (beta = 0.280, $P = 0.008$), as was the regression coefficient between C-Ach and WUN Q_R (beta = 0.192, $P = 0.01$) (Fig. 7D). The total effect and the direct effect were not statistically significant (beta = 0.068, $P = 0.365$; beta = 0.014, $P = 0.850$). The bootstrapped indirect effect was $(0.280) \times (0.192) = 0.054$, and the 95% confidence interval ranged from 0.006 to 0.130. Thus, the indirect effect was statistically significant ($P = 0.018$).
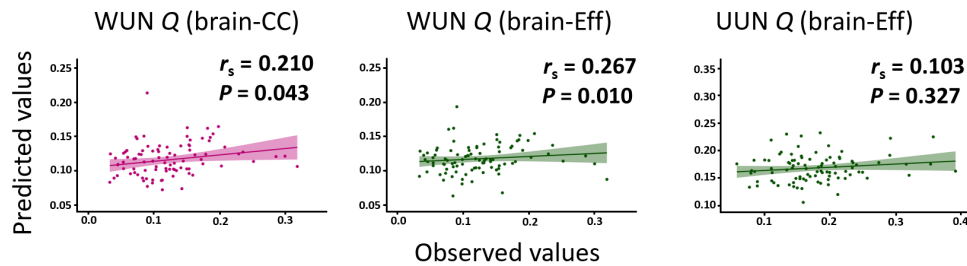
Fig. 6. Predicted and observed SemNet metrics from resting-state connectivity. The plots show the Spearman correlations between the predicted values (*y* axis) and observed values (*x* axis) of SemNet metrics based on resting-state brain connectivity. Green plots are presented for brain-Eff and magenta ones for brain-CC. In the upper-right side of each plot, we present the r_s and the *P* values.
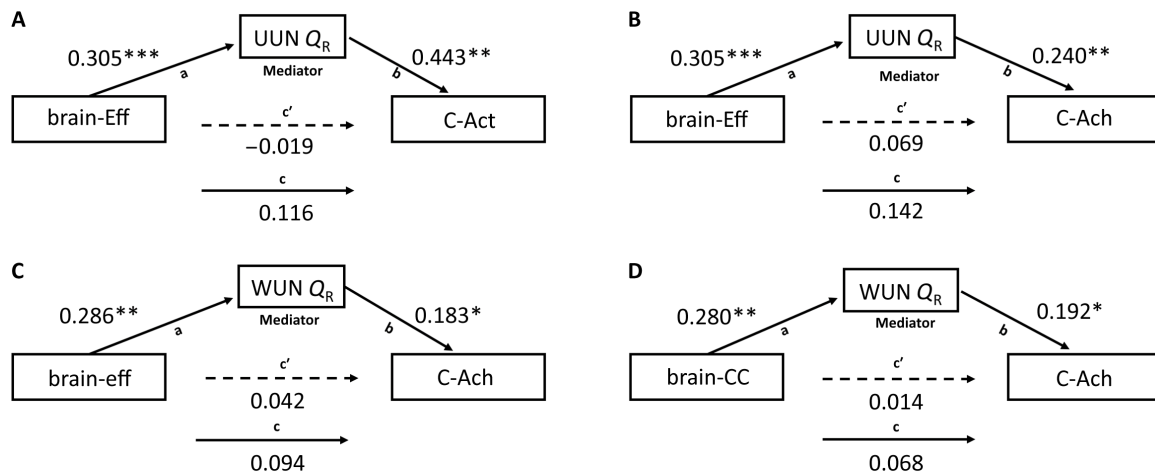

Fig. 7. Mediation analyses. Results of the mediation models are presented in path diagrams. Each diagram indicates the beta weights of the regression coefficients, with the brain metrics of the model network (brain-Eff and brain-CC) as the independent variable (predictor), SemNet metrics as the mediator (UUN Q_R and WUN Q_R), and real-life creativity (C-Act and C-Ach) as the dependent variable (outcome). The total effect is indicated by path c, the direct effect by path c', and the indirect effect is given by the product of path a and path b. The indirect effect was significant in all the reported mediations. (**A**) The mediating role of UUN *Q* on the relationship between the brain-Eff of the brain functional network predicting it and C-Act. (**B**) Mediating role of UUN *Q* between the brain-Eff of the brain network predicting it and C-Ach. (**C**) Mediating role of the weighted network WUN *Q* on the relationship between the brain-Eff of the functional connectivity of the negative model network predicting it and C-Ach. (**D**) Mediating role of WUN *Q* on the relationship between the brain-CC of the functional connectivity of the negative model network predicting it and C-Ach. *$P < 0.05$, **$P < 0.01$, and ***$P < 0.001$.

Hence, SemNet WUN *Q* mediated the link between the efficiency (brain-Eff) and the clustering coefficient (brain-CC) of functional brain connectivity and real-life creative achievements (C-Ach): The higher the efficiency and clustering of the negative model network that predicted WUN *Q*, the lower SemNets *Q*, and the higher the real-life creative achievements. In summary, individual SemNets *Q* measured in WUN and UUN mediated the relationship between brain functional connectivity and real-life creativity.

DISCUSSION
Our results advance our knowledge on the role of semantic memory structure in creativity by showing how individual SemNet properties predict real-life creative activities and achievements in various domains. In addition, our neuroimaging results reveal patterns of brain functional connectivity predicting individual differences in real-life creativity via these quantitative properties of semantic memory structure. A few studies had shown a link between creative performance and semantic memory structure, and others identified brain connectivity profiles predictive of creative abilities. Here, we combined and extended these approaches to investigate the neural and cognitive basis of creative behavior in real life. Recently developed computational approaches (*41*, *42*) allowed us to predict complex cognitive functions from brain connectivity and to explore the organization of semantic memory at the individual level using SemNets (*5*, *13*, *26*). We show that brain connectivity during semantic relatedness judgments predicted individual differences in the modularity of SemNets that was identified as a behavioral marker of individual differences in real-life creativity. Specifically, more efficient and denser functional connectivity between the default, control, salience, motor, and visual networks predicted a more integrated semantic memory structure (less modular SemNets) that, in turn, predicted more creative behaviors. These findings provide an unprecedented understanding of how brain and semantic memory networks relate to real-life creative behavior.

According to the associative theory of creativity (*6*), highly creative individuals are characterized by a more flexible organization of concepts in their semantic memory, allowing them to more easily retrieve remote associations (*4*, *17*, *49*). A recent study revealed the mediating role of associative abilities between semantic memory

structure and creativity as measured by verbal divergent thinking tasks (5). Here, we show that individual-based semantic memory network properties also relate to real-life creativity: Individuals with a more compact and less modular organization of their semantic memory exhibit more creative accomplishments. Part of this effect was consistent across both indicators of creative behavior (C-Act and C-Ach were predicted from Q), while there were also subtle differences (C-Act was additionally predicted by ASPL), which indicates differences in reliance on semantic memory structure in different realization of real-life creative behavior. This finding was also consistent using two different thresholding methods for the SemNet (WUN and UUN) and remained significant when controlling for sex, education, and IQ. Our finding is in line with the previously reported relationship between semantic associative ability and creative behavior in real life (11, 15) and additionally shows how this relationship could be explained by individual differences in semantic memory structure, in particular, as reflected by SemNet modularity. Less modular networks may allow more flexible thinking, with a higher connectivity between weakly related elements facilitating their combination. Overall, our results reveal that semantic memory structure assessed at the individual level is a cognitive marker of real-life creativity and that a less segregated (less modular) SemNet structure is especially important for creative behavior.

Furthermore, we show that semantic memory structure mediates the effect of brain functional connectivity on real-life creative activities and achievements. The higher the efficiency and overall connectivity of the brain predictive network, the more flexible the SemNet (characterized by being more compact and less modular), and the more creative the participant is. Previous studies exploring the cognitive processes involved in creativity have revealed brain regions and functional networks associated with different creativity tasks (30, 32). The use of SemNets allowed us to explore mechanisms that appear more broadly relevant to the associative basis of creative cognition, avoiding the specificities of association tasks. Using a whole-brain functional connectivity approach, we identified the task-based functional connectivity patterns related to semantic memory network properties predicting creative activities and achievements. An internal validation of the predictive models using resting-state fMRI data suggests that the whole-brain predictive models that we built in the task-based functional connectivity are robust and generalizable to the individual's resting-state functional connectivity. However, while the validation was significant for the CPM predictions of WUN metrics, this did not apply to UUN metrics, which remains to be explained.

The predictive patterns included functional connections distributed across the whole brain, the densest being observed between brain networks previously linked to creativity (30, 31, 36, 50, 51). The major contributions to the prediction of creativity resulted from functional links between control and default mode networks, within salience network, and between somatomotor and visual networks. The default mode network has been associated with several aspects of cognition involving heteromodal memory representation including self-generated thoughts and spontaneous associations (17, 19), as well as control-demanding activities such as semantic goal maintenance (40). The control network is associated with controlled processes such as attentional control, working memory, inhibition, memory retrieval, and flexibility, which are necessary to accomplish the objectives of a specific task (52). The functional coupling between control and default mode networks has been reported in relation to

creative cognition in several studies (30, 31). In addition, higher intrinsic connectivity of semantically relevant control and default mode network regions was associated with better performance in a task largely similar to the remote associate task commonly used to study creativity (37). Hence, our results can be interpreted in light of the controlled semantic cognition framework (38), where conceptual representations interact with control processes when semantic retrieval is tailored to suit the circumstances. In addition to control and default mode networks, the salience network has also been reported to play a critical role in creativity. It has been associated with attentional switching and detection of salient external or internal stimuli and appears to play a role in triggering the engagement of control and default mode networks during creativity tasks (30). Overall, our findings indicate the relevance of functional coupling within and between control, default, and salience networks for real-life creativity and characterize its role in semantic memory properties captured by SemNet metrics.

A considerable number of functional connections between somatomotor and visual networks also contributed to the prediction of creativity via SemNet properties. Both networks have been associated with creativity in previous studies (36, 42), but independently. The motor system has been related to creativity as measured by different approaches, including verbal creativity, music improvisation, and visuospatial creativity (36, 50). The brain regions of visual networks also appear to play an important role mainly in visuospatial creativity (50), and their activation was previously correlated with higher creative achievements (53). A recent study using the CPM approach showed the contribution of visual networks in the overlapping brain patterns predicting creativity and intelligence (42). Our study adds to this previous work by showing the involvement of the coupling of motor and visual networks in creativity. The role of motor and visual regions in creativity can be plural. In the context of our RJT task used to estimate SemNets, semantic relatedness judgments may evoke visual representations and motor experiences associated with the concepts (38). It is then possible that less modular SemNets reflect less segregated motor and visual memory contents in more creative individuals than in less creative ones and closer connections between remote concepts in memory. In addition to the connectivity between control, default, and salience networks, the current findings also shed new light on the contribution of the coupling between regions of the visual and motor networks for creativity.

To further characterize the predictive patterns of functional brain connectivity, we identified the nodes with the highest number of connections being localized in the medial prefrontal cortex, insula, the extrastriate inferior region, parietal medial and temporoparietal regions, and temporal pole in the right hemisphere. Most of these regions have been reported to play a role in creative cognition. In a brain lesion study, the medial prefrontal cortex of the default mode network has been shown to be relevant in associative processes underlying creative cognition (17). Moreover, this brain region and the insula of the salience network have been highlighted as essential regions for verbal creativity (30, 31). The right lingual gyrus, part of the extrastriate cortex, is also recruited in verbal creativity tasks (32) in relation to the originality of semantic associations (15) and to internally directed attention reflecting increased visual imagery (54). Other temporal areas, including the right temporoparietal regions and temporal pole, have been associated with verbal and visual creativity (55), including insight problem solving (56), mental imagery (57), and creative achievements (58). The involvement

of the anterior temporal pole is consistent with its role as a semantic hub (38) and in abstract thinking and categorization (59, 60).

One unexpected result is that the highest-degree brain nodes related to real-life creativity were distributed within the right hemisphere. Previous analyses reported a left dominance for creativity regions in functional (32, 34), connectivity (31), and structural (61) imaging studies. Most verbal creativity tasks highlight the critical role of brain regions of the left hemisphere, particularly in the prefrontal and temporal cortices, possibly related to linguistic/semantic processing (32, 62). Here, we also identified left-lateralized highly connected nodes contributing to the prediction of differences in real-life creativity in the left ventral prefrontal cortex of the control network and in the insula of the salience network, regions that have been shown critical for verbal creativity (18, 31), as well as in regions underlying semantic cognition (38–40).

Yet, the right dominance of the predictive patterns in our study was unexpected because our study focused on the semantic basis of creative cognition and used a verbal task. The strong engagement of the right hemisphere might be related to the process of judging remote concepts during the RJT. Previous studies have indeed associated the right hemisphere with a relatively coarser semantic coding (63) and the activation of broader semantic fields by words or contexts (64). Moreover, the engagement of broad associative processes in the right hemisphere has been related to hemispheric brain asymmetries in dopamine function (65). More creative individuals may rate distant words as more related during the RJT than less creative ones, which might rely on a higher functional connectivity with or within the right hemisphere. Hence, these findings show that diverse regions previously reported as central to creative cognition participate together in the predictive connectivity patterns of real-life creativity through a less segregated organization of semantic memory (lower SemNet modularity). Whether and how SemNet modularity reflects remote thinking that would rely more specifically on the right functional connectivity remain to be addressed in future studies.

Last, the current SemNets-related results relate to recent neuroimaging studies exploring the associative processes of creativity (19, 33). Higher associative abilities in a free chain association task have been related to higher resting-state functional connectivity within the default mode network (19) and to larger gray matter volume in the left posterior inferior temporal gyrus (33). In both studies, higher associative abilities mediated the relationship between a priori–selected regions of the brain and creativity. One recent study showed that efficiency in SemNets mediated the link between gray matter volume in the left temporal pole and a divergent thinking task (28). Our findings provide additional knowledge in several critical ways. First, by using SemNets, we were able to estimate ones' structure of semantic memory, which offers some mechanistic perspective on remote and associative thinking and reveals the importance of a less segregated structure of semantic memory in creativity. Second, our findings highlight the role of semantic memory structure not only in creative thinking as assessed in the laboratory, and previously shown (5, 13, 14, 26), but also in relation to real-life creative activities and achievements. Third, we used a whole-brain approach without focusing on a priori regions or networks. Last, we explored functional connectivity not during rest, but during the RJT, while all participants performed the same trials. This approach minimized individual differences in mental activity during scanning. It importantly provided

access to the functional connectivity configuration that occurs during semantic relatedness judgments that reflect semantic associations. Overall, the unprecedented combination of recently developed network approaches allowed us to demonstrate that brain functional connectivity profiles predict creative behavior mediated by semantic memory structure, thereby characterizing what aspects of brain and memory structure are relevant to support creative behavior. More generally, our research jointly considers neurophysiological, psychological, and behavioral levels, uniquely enhancing our understanding of how complex creative behavior manifests across neural and cognitive mechanisms. A recent bio-psycho-behavioral model of creativity (66) highlighted how only research that systematically cuts across these multiple levels of analysis could advance our understanding of real-life creativity.

Some limitations to this study need to be acknowledged. First, our sample is relatively small and the use of additional external validation would add strong support to our findings. In addition, we observed significant sex differences in some SemNet metrics in WUN and UUN. We performed analyses at the behavior and brain level to control for the impact of sex differences (as well as education and IQ) on our results, which supported the robustness of the findings. However, the sample size did not allow us to explore the CPM predictions separately for women and men. Thus, future studies should explore how SemNet metric differences between women and men influence creative abilities. Second, we used the SemNet approach that is rooted in the associative theory of creativity (6) to estimate individual semantic memory networks on the basis of relatedness judgments of word pairs. The RJT-based SemNet metrics may not capture all the complexity of associative thinking. Thus, more work is needed to replicate our findings, using alternative methods to estimate an individual's SemNets. It further remains to be explored how the results generalize across different performances in distinct creative domains. Third, the stability of the SemNet properties with different sets of words remains to be properly tested. However, comparing the current results to previous studies that used the RJT with different words in different languages to estimate individual SemNets provides indirect support for the reliability of network solutions (5, 13). Moreover, a recent study explored SemNet metrics across two time points without any manipulation task in between for a baseline group of the study. The authors found no differences across the two SemNets in this group, thus providing further support for the stability of these network estimation approaches (67). Last, real-life creativity is not exclusively predicted by semantic memory. Many other internal and external factors are important to creativity, such as personality, motivation, emotions, and environment (1, 68, 69). Despite these other potential dimensions and sources of variability, the brain connectivity patterns allowed us to predict real-life creativity through the individual differences in semantic memory structure, uncovering its strong influence on creative activities and achievements.

In conclusion, our findings substantially advance our understanding of the cognitive and neural basis of creativity by revealing the brain connectivity profile that characterizes higher creativity in real life and by identifying one of the underlying cognitive mechanisms anchored in semantic memory structure. Our study combining advanced network-based methods in unprecedented ways also illustrates how the organization of cognitive and neural networks can relate to each other, opening up exciting new avenues for scientific inquiry.

MATERIALS AND METHODS

Participants

All participants were French native speakers, right handed, and with normal or corrected-to-normal vision. A total of 101 healthy participants (48 women) aged between 22 and 40 years (mean 25.6 years ± SD = 3.7) with formal years of education between 12 and 22 years (mean 16.6 years ± SD = 1.5) were recruited via the Relais d'information sur les sciences de la cognition (RISC) platform (www.risc.cnrs.fr). Participants declared no history of neurological or psychiatric disease, no evolutive neuropsychiatric condition, no psychotropic medication, and no drug abuse or cognitive difficulties. In total, eight participants were excluded from the fMRI analysis: Six participants were excluded because of the discovery of MRI brain abnormalities, one participant fell asleep during the acquisition of the data (precluding the analysis of both MRI and RJT data), and another participant had a claustrophobia episode at the beginning of the MRI scanning. The latter participant performed the RJT task outside the scanner and, because his data did not deviate with respect to the group (scores and metrics were within ±2 SDs of the group mean), it was kept in the behavioral analyses (also see table S2 for the results without this participant). The final sample was hence composed of 94 participants aged between 22 and 37 years (mean 25.4 ± 4.2; 44 women) in behavioral analyses and 93 participants in the fMRI analyses (mean age 25.4 ± 3.4; 44 women). An approved French ethics committee approved the study. After being informed of the study, the participants signed a written consent form. They were paid 140 euros for their participation (that included an MRI session lasting almost 2 to 3 hours of cognitive tests) and were reimbursed for transportation when relevant. Cognitive testing included tasks that are outside the scope of this article.

General procedure

Participants underwent a task-based fMRI session during which they performed the RJT. Several training tasks were conducted before acquiring the fMRI data, first outside the scanner, then in the scanner. The training included a motor training task to become familiar with giving responses using the MRI-compatible trackball on a visual scale in the RJT and a task training to get familiar with the actual task. The task training was similar to the actual task but using different stimuli. In addition, all words used in the RJT were displayed to participants to check that they were familiar with all of them (details of the task training are described in section S1). After the fMRI session, participants completed a set of creativity tasks on a computer outside the scanner that lasted around 3 hours.

Relatedness judgment task
Task and material description

The RJT has been used to estimate individual-based SemNets and to explore the structure of semantic memory (5, 13, 26). The task requires participants to judge the relatedness of all possible pairs of words from a list of cue words. These judgments are then used to estimate an individual's semantic memory network of these words. The selection of the RJT stimulus words used in our study is detailed by Bernard *et al.* (26) (a summary is given in section S2). Briefly, we first created a French SemNet, based on French verbal association norms (http://dictaverf.nsu.ru/dictlist), where the nodes represent the words and the links were weighted by the normative associative strength between words. Next, we computed the shortest path between words, and the minimal number of links between

each pair was considered as the theoretical semantic distance between the words. Last, we applied a computational method to select the RJT words that optimized the repartition of the theoretical semantic distance between all possible pairs of these words. The optimal solution included 35 words, resulting in a total of 595 word pairs that represented the 595 RJT trials.

Each trial began with the displaying word pair on the screen along with a visual scale below ranging from 0 (unrelated) to 100 (strongly related). The stimuli were displayed for 4 s in total, divided into a reflection period of 2 s to ensure a comparable minimum judgment time and a response period of 2 s. During the first 2 s, the participants studied the word pair but could not move the slider yet. Two seconds after stimuli onset, the response period began, the cursor appeared in the middle of the visual scale, and the participants were allowed to move the slider on the visual scale to indicate their rating using a trackball. Participants were instructed to validate their response by clicking the left button of the trackball. The position of the cursor on the scale at the moment of the validation was recorded as the relatedness judgment. When participants did not validate their response, we recorded the slider position at the end of the 2-s response period. After the response period, a blank screen was shown during the intertrial interval jittered from 0.3 to 0.7 s (steps = 0.05; Fig. 1A).

Task trials were distributed into six runs composed of 100 trials each, except for the last run (95 trials). Each run consisted of four blocks of 25 trials each (except the last block of the sixth run, with only 20 trials), separated by a 20-s rest period with a cross fixation on the screen. Trials were pseudo-randomly ordered within blocks, such that each block contained a similar proportion of word pairs of each theoretical semantic distance. At the beginning and end of each run, participants had a 10-s rest period with a cross fixation on the screen. During the last 2 s of cross fixation periods, the cross changed color, warning the participant that the task was about to start. Participants had a self-paced break inside the scanner between runs.

Assessment of individual SemNet structure

Building individual SemNets. The relatedness ratings given by the participant to each pair of words was used to weigh the links of the individual SemNet where each word is a node. We represent each of these networks as a 35 by 35 matrix with one column and one row for each word, and cell values correspond to the judgment given by the participant during the RJT (Fig. 1B). On the basis of previous studies and on our pilot study (5, 13, 26), we estimated two types of networks, WUN and UUN (Fig. 1C), which vary on the type of threshold applied to the network. The WUN is a more informed type of the SemNet because it keeps the weights of all links between the words. The UUN is a less informed approach, retaining links above a defined threshold, and the links with a weight below the threshold are removed. We defined the threshold as a rating value of 50 (the middle of the visual scale) to keep the links between words that were considered moderately or highly associated by the participants. The weights of the remaining links are uniformly set to 1.

Calculation of the individual SemNet metrics. We estimated the properties of the individual SemNet independently for the UUN and the WUN graphs. On the basis of previous studies relating SemNet to creative abilities (5, 13, 14, 24, 26), we computed the SemNet metrics that have been correlated to creativity: ASPL, CC, Q, and S metrics. The ASPL is the average shortest number of steps needed to be taken between any pair of nodes. In SemNets, path

length reflects how related two concepts are to each other (*70*). The clustering coefficient (CC) measures the network's connectivity. It refers to the probability that two neighbors of a node will be neighbors themselves. In SemNets, higher CC relates to a higher overall relatedness between concepts. Modularity (*Q*) measures how a network is divided (or partitions) into smaller subnetworks; a higher *Q* relates to more subcommunities in the network (*71*). These subcommunities can reflect semantic categories in a SemNet. In creativity research, for example, more creative individuals often exhibit a more connected (higher CC), less segregated (lower ASPL and *Q*) SemNet than less creative individuals, and these differences were related to flexibility of thought (*24*). The small-worldness (*S*) property of the network is calculated as the ratio between CC and ASPL and describes how much the nodes that are not directly linked can be reached through connections between their neighbors. In SemNets, higher *S* has been linked to higher flexibility of thought (*14*). The computations were performed in MATLAB, via the Brain Connectivity Toolbox (*72*) (www.mathworks.com).

Assessment of real-life creativity

Outside the scanner, we used the ICAA questionnaire (*29*) to assess the real-life creative activities and achievements across eight different creative domains (i.e., literature, music, art and crafts, creative cooking, sport, visual arts, performing arts, and science and engineering). The creative activities (C-Act) score reflects the frequency in which participants engaged in various creative activities. Six different questions were posed for each domain, and participants reported the frequency with which they engaged in each activity during the last 10 years using a scale ranging from 0 (never) to 4 (more than 10 times). The maximum score for each domain is 24 points. For each participant, the final domain-general score of C-Act was the sum of the creative activities across all activities of the eight different domains. The creative achievements (C-Ach) score estimated the level of achievement acquired in a creative domain. Ten different levels of achievement were included for each domain going from 0 (never engaged in this domain) to 10 (I have already sold some of my work in this domain). The maximum score for each domain is 55 points. For each participant, the final domain-general score of C-Ach was the sum of the scores across the eight different domains. Overall, creative activities capture the differences in the frequency of everyday creative behaviors, whereas creative achievements capture differences in publicly acknowledged creative accomplishments (*29*). A summary of the questions is reported in the Supplementary Materials (section S3), and the descriptive statistic for each specific domain explored in the ICAA is presented in the Supplementary Materials (table S3).

Relationships between individual SemNet metrics and creativity

We explored whether individual SemNet properties were predictive of real-life creative activities (C-Act) and achievements (C-Ach; Fig. 1E). In independent analyses, we performed linear regressions using leave-one-out cross-validations to predict C-Act and C-Ach scores for each of the SemNet metrics (ASPL, CC, *Q*, and *S* of WUN and UUN SemNets). The analyses consisted of building a predictive linear model iteratively in $N - 1$ participants using their SemNet metrics (e.g., WUN *Q* SemNet metric) and testing it in the left-out participant. The model was applied on the SemNet metric of the left-out participant to compute a predicted value of the ICAA scores. The

significance of the prediction was evaluated via Spearman correlations between the predicted and the observed creativity scores. When the correlations between observed and predicted values were positive with $P < 0.05$, we assessed its statistical significance using 1000-iteration permutation testing. We report the rho coefficient and the *P* value of the permutation test. Note that Spearman correlations are used for behavioral analyses as creative activities and achievements are typically skewed (*73*). We also ran Spearman correlations between SemNet metrics and ICAA scores to better represent the statistical association between the different SemNet metrics and creativity (Table 1). In addition, we explored the correlations between SemNet metrics and creativity and the following factors: age, education, sex, and IQ. As a proxy of the IQ, participants performed the matrix reasoning subtest of the Wechsler Adult Intelligence Scale test. The results of these correlations are reported in the Supplementary Materials (table S1). The prediction models of the significant results were reanalyzed by controlling for the factors that significantly correlated with SemNet metrics or creativity scores (fig. S1).

MRI data acquisition and preprocessing

Neuroimaging data were acquired on a 3T MRI scanner (Siemens Prisma, Germany) with a 64-channel head coil. Six functional runs were acquired during each six task runs using multi-echo echo-planar imaging (EPI) sequences. No dummy scan was recorded during the acquisition; therefore, we did not discard any volume. Each run included 335 whole-brain volumes acquired with the following parameters: repetition time (TR) = 1600 ms; echo times (TE) for echo 1 = 15.2 ms, echo 2 = 37.17 ms, and echo 3 = 59.14 ms; flip angle = 73°; 54 slices, slice thickness = 2.50 mm; isotropic voxel size of 2.5 mm; Ipat acceleration factor = 2; multiband = 3; and interleaved slice ordering. After the EPI acquisitions, a T1-weighted structural image was acquired with the following parameters: TR = 2300 ms, TE = 2.76 ms, flip angle = 9°, 192 sagittal slices with a 1-mm thickness, isotropic voxel size of 1 mm, Ipat acceleration factor = 2, and interleaved slice order. A resting-state fMRI session of 15 min (570 volumes) followed with the same parameters of acquisition as the task runs.

The preprocessing of the on-task fMRI data was performed for each run separately and for the resting-state data using the afni_proc.py pipeline from the Analysis of Functional Neuroimages software (AFNI; https://afni.nimh.nih.gov). The different preprocessing steps of the data included despiking, slice timing correction, and realignment to the first volume (computed on the first echo). We then denoised the preprocessed data using the TE-dependent analysis of multi-echo fMRI data (TEDANA; https://tedana.readthedocs.io/en/stable/), version 0.0.9 (*74*). The advantage of using multi-echo EPI sequences is that it allows better cleaning of the data by assessing the BOLD and non-BOLD signal through the independent component analysis (ICA)–based denoising method, improving the reliability of the functional connectivity–based measurement (*75*). The TEDANA pipeline consisted first of an optimal combination of the different echo time series. Then, the dimensionality of the optimally combined data is reduced through the decomposition of the multi-echo BOLD data using principal components analysis and ICA. TEDANA then classifies the resulting components as BOLD or non-BOLD. The exclusion of the non-BOLD components allowed the removal of thermal and physiological noise such as the artifacts generated by the movements, respiration, and cardiac activity. The resulting denoised data were co-registered on the T1-weighted structural image using the Statistical Parametric Mapping (SPM) 12 package running

in MATLAB (MATLAB R2017b, The MathWorks Inc., USA). We then normalized the data to the Montreal Neurological Institute template brain, using the transformation matrix computed from the normalization of the T1-weighted structural image, performed with the default settings of the computational anatomy toolbox (CAT 12; http://dbm.neuro.uni-jena.de/cat/) (76) implemented in SPM 12. The resulting denoised and normalized images from the task-based fMRI data were then entered in a general linear model in SPM to covary out the task-related signal from each run. In this analysis, we entered 24 motion parameters (standard motion parameters, first temporal derivatives, standard motion parameters squared, and first temporal derivatives squared) and the onsets and durations of each task-related event (reflection period, response period, intertrial interval, cross fixation periods, and change of the cross fixation color) as confounds that were regressed from the BOLD signal. We standardized and detrended the residuals of this model for each run and then concatenated the six runs, removing the rest periods between runs (six volumes in total). This final dataset composed of the six task-run residuals concatenated was used as input for the subsequent task-based functional connectivity analyses.

Building task-based and resting-state functional connectivity matrices

Calculation of the task-based and resting-state functional connectivity matrices for each participant was performed using Nilearn v0.3 (77) in Python 2.7 (https://ir.cwi.nl/pub/5008). We used the Schaefer brain atlas to define our regions of interest (ROIs) that consisted of 200 ROIs distributed into 17 functional subnetworks than can be summarized in eight main functional networks (43). For each ROI, we extracted the BOLD signal during the RJT (averaged across voxels) and computed the Pearson correlation coefficients of all pairs of ROIs. As a result, we obtained for each participant a 200 by 200 matrix with the correlation coefficients between all ROIs. These matrices were z-Fisher–transformed and rescaled in the range of −1 to 1 for the subsequent analyses. This matrix corresponds to the functional connectivity network of each participant in which ROIs are the nodes and correlation coefficients the links.

A CPM approach

We used a CPM approach (31, 41) to explore how SemNet properties can be predicted from functional connectivity patterns during the RJT task. We focused the CPM analyses on the SemNet metrics that predicted creativity scores following the method described by Shen *et al.* (41) (Fig. 3). We used a leave-one-out cross-validation that consisted in building the model iteratively on $N-1$ participants and test the prediction on the left-out participants.

Because head motions during the fMRI acquisition can affect the CPM results, we verified that there was no correlation between motion patterns during the fMRI acquisition and the SemNet metrics. We estimated the mean framewise displacement (FD), which is the sum of the absolute values of the derivatives of the six realignment parameters (78), and computed Spearman correlations between the mean FD and all SemNet metrics. The correlations revealed no significant correlation between the motion patterns and WUN ASPL ($r = -0.052$, $P = 0.622$), WUN Q ($r = 0.133$, $P = 0.203$), and UUN Q ($r = 0.127$, $P = 0.225$).

The first step of the CPM consists of selecting the significant features of brain connectivity to build the "model brain networks." In the training set ($N-1$), we selected the links of the functional connectivity matrix (correlation coefficients between the ROIs) that significantly correlated with the tested SemNet metric (threshold $P < 0.05$) either positively (the positive model network) or negatively (the negative model network) across participants (Fig. 3, A and B). Because SemNet metrics had non-Gaussian distributions, we used Spearman correlations. In these model networks of brain connectivity, negative links were removed (79). We normalized the values of the links (i.e., the correlation coefficients between ROIs) to have the same range of values for the calculation of the brain networks in the following step.

The second step consists in estimating functional connectivity properties within each participant's positive and negative model networks. This is one amendment from the classical protocol (41) to better take into account the structural properties of functional brain connectivity patterns. Instead of summing the links in the model networks (as in the classical CPM method), we estimated the network properties of the positive and the negative model networks using network metrics (Fig. 3C). We computed two different whole-brain model network metrics: (i) network efficiency (brain-Eff), measuring rapid and efficient integration across the network (80), and (ii) CC (brain-CC), key property describing a small-world properties network characterizing the human brain (44). The brain-Eff metric was calculated as the average of the inverse shortest path length. The computation of the brain-CC metrics was similar to the CC of the SemNet described above in the "Calculation of the individual SemNet metrics" section.

The third and fourth steps consist in building the predictive model using the computed network properties and then applying it to a novel participant (the left-out one for each iteration; Fig. 3D). These steps were conducted separately for each SemNet metric and each model network property. We built a single linear model combining the network metric of the positive and negative model networks of $N-1$ participants as predictors of a given SemNet metric. The mean FD was included in the model to deal with possible effects of the head motion related to fMRI acquisition on the CPM process. At each iteration, we computed the network metric of the positive and the negative model networks in the left-out participant. We used these values as predictors in the linear model to compute its predicted value of the SemNet metric tested.

The final step evaluated the predictive model by performing a Spearman correlation between the predicted and the observed SemNet metric. The correlations near or below zero indicate model failure (41). Because we used within-dataset cross-validation, for the significant predictions, it was necessary to evaluate the predictive power of the CPM using permutation testing to assess the statistical significance of the results. To this end, we randomly shuffled the values of the SemNet metric 1000 times, and we ran the new random data through the pipeline of our predictive model to generate an empirical null distribution and estimate the distribution of the test statistic given by the correlation between predicted and observed values. In addition, the prediction models of the significant results were analyzed by controlling for the factors that significantly correlated with SemNet metrics or creativity scores (table S1). To perform this analysis, we varied the third step of our CPM analysis by including sex, education, and IQ measures to the predictive model. We evaluated the predictive model by performing a Spearman correlation between the predicted and the observed SemNet metric (fig. S2). The CPM analyses were performed using the MATLAB Statistical Toolbox (MATLAB R2020a, The MathWorks Inc., USA). The pipeline for the CPM is an adaptation from the protocol by Shen *et al.* (41).

Functional anatomy of the predicting brain model networks

To explore the patterns of connectivity predicting the SemNet metrics, we characterized the main nodes and links of the significant model networks. We examined the distribution of the connections at the lobar level (between and within brain lobes) and at the intrinsic network level (within and between the eight main functional networks defined by the Schaefer atlas). Last, we explored the brain distribution of the six highest-degree nodes (i.e., ROIs), which are the nodes with the highest number of connections. Because of the nature of the cross-validation approach (running one model for each iteration on $N − 1$ participants), each iteration likely resulted in slightly different links in the model networks. Therefore, we considered the links that were shared between all iterations. The data visualization and plots were performed using BioImage Suite Web 1.0 (https://bioimagesuiteweb.github.io/webapp/connviewer.html), BrainNet viewer (81) (www.nitrc.org/projects/bnv/) in MATLAB, and custom scripts in RStudio version 1.3.1056.

Internal validation: Prediction of creativity-related SemNet properties from resting-state functional connectivity

To generalize our predictive models, and as an internal validation, we performed the prediction of the SemNet metrics from the resting-state functional connectivity. To this end, we used the on-task functional connectivity properties (brain-Eff and brain-CC) within each participant's positive and negative model networks to build the predictive model. We applied the predictive model in the resting-state data of the participants using the resting-state functional connectivity properties within each participant's positive and negative model networks during the resting-state acquisition (31). As for task-based analyses, mean FD was included in the models. The Spearman correlations between the predicted and the observed SemNet metrics were estimated to evaluate the prediction.

Mediation analysis

To test whether the patterns of functional connectivity that predict SemNet properties are also relevant for real-life creativity, we ran mediation analyses. For significant CPM predictions, we tested whether the SemNet metrics mediated the relationship between the patterns of brain functional connectivity and creativity. As for the CPM analyses, the mediation analyses focused on the SemNet metrics that correlated with creativity scores. Hence, they explored an indirect effect of the functional brain connectivity on creativity through the SemNet properties.

The mediation analysis (82) consisted in calculating the product of (i) the regression coefficient of the regression analysis on the independent variable (i.e., brain functional connectivity metric, brain-CC, or brain-Eff of the positive or the negative model networks) to predict the mediator (i.e., SemNet metrics) and (ii) the regression coefficient of the regression analysis on the mediator to predict the dependent variable (i.e., creativity score) when controlling for the independent variable. We also calculated the regression coefficient of the regression analysis on the independent variable to predict the dependent variable without controlling for the mediator (total effect) and when controlling for it (direct effect; Fig. 7). The indirect effect was calculated as the product of path a and path b. All the variables entered in the mediation analyses were normalized. To decrease the impact of the skewness, we log-transformed the variables with skewed distributions (C-Ach, C-Act, and SemNet metrics). The variables that had a negative correlation with creativity were reversed (multiplied by −1). The selection of the positive or the negative network to be used on the mediation analysis depended on which of them is expected to be positively correlated to the creativity score. We tested the significance of the indirect effect using bootstrapping method, computing unstandardized indirect effects for each 5000 bootstrapped samples, and the 95% confidence interval was computed by determining the indirect effects at the 2.5th and 97.5th percentiles. The mediation analyses were performed using the PROCESS macro (82) in SPSS 22.0 (IBM Corp. in Armonk, NY, USA).

SUPPLEMENTARY MATERIALS

REFERENCES AND NOTES

1. S. Mastria, S. Agnoli, M. Zanon, T. Lubart, G. E. Corazza, in *Exploring Transdisciplinarity in Art and Sciences*, Z. Kapoula, E. Volle, J. Renoult, M. Andreatta, Eds. (Springer International Publishing, 2018), pp. 3–29.
2. R. E. Beaty, P. J. Silvia, E. C. Nusbaum, E. Jauk, M. Benedek, The roles of associative and executive processes in creative cognition. *Mem. Cognit.* **42**, 1186–1197 (2014).
3. R. E. Beaty, D. C. Zeitlen, B. S. Baker, Y. N. Kenett, Forward flow and creative thought: Assessing associative cognition and its role in divergent thinking. *Think Skills Creat.* **41**, 100859 (2021).
4. M. Benedek, T. Könen, A. C. Neubauer, Associative abilities underlying creativity. *Psychol. Aesthet. Creat. Arts* **6**, 273–281 (2012).
5. L. He, Y. N. Kenett, K. Zhuang, C. Liu, R. Zeng, T. Yan, T. Huo, J. Qiu, The relation between semantic memory structure, associative abilities, and verbal and figural creativity. *Think. Reason.* **27**, 268–293 (2021).
6. S. A. Mednick, The associative basis of the creative process. *Psychol. Rev.* **69**, 220–232 (1962).
7. E. Volle, in R.E. Jung & O. Vartanian (Eds.), *The Cambridge Handbook of the Neuroscience of Creativity* (Cambridge Univ. Press, 2018), pp. 333–360.
8. E. Rossmann, A. Fink, Do creative people use shorter associative pathways? *Personal. Individ. Differ.* **49**, 891–895 (2010).
9. O. Vartanian, C. Martindale, J. Matthews, Divergent thinking ability is related to faster relatedness judgments. *Psychol. Aesthet. Creat. Arts* **3**, 99–103 (2009).
10. K. Gray, S. Anderson, E. E. Chen, J. M. Kelly, M. S. Christian, J. Patrick, L. Huang, Y. N. Kenett, K. Lewis, "Forward flow": A new measure to quantify free thought and predict creativity. *Am. Psychol.* **74**, 539–554 (2019).
11. R. Prabhakaran, A. E. Green, J. R. Gray, Thin slices of creativity: Using single-word utterances to assess creative cognition. *Behav. Res. Methods* **46**, 641–659 (2014).
12. D. Bendetowicz, M. Urbanski, C. Aichelburg, R. Levy, E. Volle, Brain morphometry predicts individual creative potential and the ability to combine remote ideas. *Cortex* **86**, 216–229 (2017).
13. M. Benedek, Y. N. Kenett, K. Umdasch, D. Anaki, M. Faust, A. C. Neubauer, How semantic memory structure and intelligence contribute to creative thought: A network science approach. *Think. Reason.* **23**, 158–183 (2017).
14. Y. N. Kenett, D. Anaki, M. Faust, Investigating the structure of semantic networks in low and high creative persons. *Front. Hum. Neurosci.* **8**, 407 (2014).
15. M. Benedek, J. Jurisch, K. Koschutnig, A. Fink, R. E. Beaty, Elements of creative thought: Investigating the cognitive and neural correlates of association and bi-association processes. *Neuroimage* **210**, 116586 (2020).
16. J. A. Olson, J. Nahas, D. Chmoulevitch, S. J. Cropper, M. E. Webb, Naming unrelated words predicts creativity. *Proc. Natl. Acad. Sci. U.S.A.* **118**, e2022340118 (2021).
17. D. Bendetowicz, M. Urbanski, B. Garcin, C. Foulon, R. Levy, M.-L. Bréchemier, C. Rosso, M. Thiebaut de Schotten, E. Volle, Two critical brain networks for generation and combination of remote associations. *Brain* **141**, 217–233 (2018).
18. M. P. Ovando-Tellez, T. Bieth, M. Bernard, E. Volle, The contribution of the lesion approach to the neuroscience of creative cognition. *Curr. Opin. Behav. Sci.* **27**, 100–108 (2019).
19. T. R. Marron, E. Berant, V. Axelrod, M. Faust, Spontaneous cognition and its relationship to human creativity: A functional connectivity study involving a chain free association task. *Neuroimage* **220**, 117064 (2020).
20. A. E. Green, K. A. Spiegel, E. J. Giangrande, A. B. Weinberger, N. M. Gallagher, P. E. Turkeltaub, Thinking cap plus thinking zap: tDCS of frontopolar cortex improves creative analogical reasoning and facilitates conscious augmentation of state creativity in verb generation. *Cereb. Cortex* **27**, 2628–2639 (2017).
21. T. Merten, I. Fischer, Creativity, personality and word association responses: Associative behaviour in forty supposedly creative persons. *Personal. Individ. Differ.* **27**, 933–942 (1999).

22. M. Benedek, A. Fink, Toward a neurocognitive framework of creative cognition: The role of memory, attention, and cognitive control. *Curr. Opin. Behav. Sci.* **27**, 116–122 (2019).

23. Y. N. Kenett, in *Exploring Transdisciplinarity in Art and Sciences*, Z. Kapoula, E. Volle, J. Renoult, M. Andreatta, Eds. (Springer International Publishing, 2018), pp. 49–75.

24. Y. N. Kenett, M. Faust, A semantic network cartography of the creative mind. *Trends Cogn. Sci.* **23**, 271–274 (2019).

25. C. S. Q. Siew, D. U. Wulff, N. M. Beckage, Y. N. Kenett, Cognitive network science: A review of research on cognition through the lens of network representations, processes, and dynamics. *Complexity* **2019**, 2108423 (2019).

26. M. Bernard, Y. Kenett, M. Ovando-Tellez, M. Benedek, E. Volle, "Building individual semantic networks and exploring their relationships with creativity," *Proceedings of the 41st Annual Meeting of the Cognitive Science Society*, A. Goel, C. Seifert, C. Freksa, Eds. (Cognitive Science Society, 2019), pp. 138–144.

27. S. Acar, M. A. Runco, Divergent thinking: New methods, recent research, and extended theory. *Psychol. Aesthet. Creat. Arts* **13**, 153–158 (2019).

28. T. Yan, K. Zhuang, L. He, C. Liu, R. Zeng, J. Qiu, Left temporal pole contributes to creative thinking via an individual semantic network. *Psychophysiology* **58**, e13841 (2021).

29. J. Diedrich, E. Jauk, P. J. Silvia, J. M. Gredlein, A. C. Neubauer, M. Benedek, Assessment of real-life creativity: The Inventory of Creative Activities and Achievements (ICAA). *Psychol. Aesthet. Creat. Arts* **12**, 304–316 (2018).

30. R. E. Beaty, M. Benedek, P. J. Silvia, D. L. Schacter, Creative cognition and brain network dynamics. *Trends Cogn. Sci.* **20**, 87–95 (2016).

31. R. E. Beaty, Y. N. Kenett, A. P. Christensen, M. D. Rosenberg, M. Benedek, Q. Chen, A. Fink, J. Qiu, T. R. Kwapil, M. J. Kane, P. J. Silvia, Robust prediction of individual creative ability from brain functional connectivity. *Proc. Natl. Acad. Sci. U.S.A.* **115**, 1087–1092 (2018).

32. G. Gonen-Yaacovi, L. C. de Souza, R. Levy, M. Urbanski, G. Josse, E. Volle, Rostral and caudal prefrontal contribution to creativity: A meta-analysis of functional imaging data. *Front. Hum. Neurosci.* **7**, 465 (2013).

33. C. Liu, Z. Ren, K. Zhuang, L. He, T. Yan, R. Zeng, J. Qiu, Semantic association ability mediates the relationship between brain structure and human creativity. *Neuropsychologia* **151**, 107722 (2021).

34. L. S. Cogdell-Brooke, P. T. Sowden, I. R. Violante, H. E. Thompson, A meta-analysis of functional magnetic resonance imaging studies of divergent thinking using activation likelihood estimation. *Hum. Brain Mapp.* **41**, 5057–5077 (2020).

35. M. Benedek, T. Schües, R. E. Beaty, E. Jauk, K. Koschutnig, A. Fink, A. C. Neubauer, To create or to recall original ideas: Brain processes associated with the imagination of novel object uses. *Cortex* **99**, 93–102 (2018).

36. H. E. Matheson, Y. N. Kenett, The role of the motor system in generating creative thoughts. *Neuroimage* **213**, 116697 (2020).

37. M. Evans, K. Krieger-Redwood, T. R. Gonzalez Alam, J. Smallwood, E. Jefferies, Controlled semantic summation correlates with intrinsic connectivity between default mode and control networks. *Cortex* **129**, 356–375 (2020).

38. M. A. L. Ralph, E. Jefferies, K. Patterson, T. T. Rogers, The neural and computational bases of semantic cognition. *Nat. Rev. Neurosci.* **18**, 42–55 (2017).

39. Z. Gao, L. Zheng, R. Chiou, A. Gouws, K. Krieger-Redwood, X. Wang, D. Varga, M. A. L. Ralph, J. Smallwood, E. Jefferies, Distinct and common neural coding of semantic and non-semantic control demands. *Neuroimage* **236**, 118230 (2021).

40. X. Wang, Z. Gao, J. Smallwood, E. Jefferies, Both default and multiple-demand regions represent semantic goal information. *J. Neurosci.* **41**, 3679–3691 (2021).

41. X. Shen, E. S. Finn, D. Scheinost, M. D. Rosenberg, M. M. Chun, X. Papademetris, R. T. Constable, Using connectome-based predictive modeling to predict individual behavior from brain connectivity. *Nat. Protoc.* **12**, 506–518 (2017).

42. E. Frith, D. B. Elbich, A. P. Christensen, M. D. Rosenberg, Q. Chen, M. J. Kane, P. J. Silvia, P. Seli, R. E. Beaty, Intelligence and creativity share a common cognitive and neural basis. *J. Exp. Psychol. Gen.* **150**, 609–632 (2021).

43. A. Schaefer, R. Kong, E. M. Gordon, T. O. Laumann, X.-N. Zuo, A. J. Holmes, S. B. Eickhoff, B. T. T. Yeo, Local-global parcellation of the human cerebral cortex from intrinsic functional connectivity MRI. *Cereb. Cortex* **28**, 3095–3114 (2018).

44. O. Sporns, The human connectome: A complex network. *Ann. N. Y. Acad. Sci.* **1224**, 109–125 (2011).

45. F. De Vico Fallani, J. Richiardi, M. Chavez, S. Achard, Graph analysis of functional brain networks: Practical issues in translational neuroscience. *Philos. Trans. R. Soc. B Biol. Sci.* **369**, 20130521 (2014).

46. R. F. Betzel, D. S. Bassett, Specificity and robustness of long-distance connections in weighted, interareal connectomes. *Proc. Natl. Acad. Sci. U.S.A.* **115**, E4880–E4889 (2018).

47. R. E. Beaty, S. B. Kaufman, M. Benedek, R. E. Jung, Y. N. Kenett, E. Jauk, A. C. Neubauer, P. J. Silvia, Personality and complex brain networks: The role of openness to experience in default network efficiency. *Hum. Brain Mapp.* **37**, 773–779 (2016).

48. Y. N. Kenett, R. E. Beaty, P. J. Silvia, D. Anaki, M. Faust, Structure and flexibility: Investigating the relation between the structure of the mental lexicon, fluid intelligence, and creative achievement. *Psychol. Aesthet. Creat. Arts* **10**, 377–388 (2016).

49. M. Benedek, A. C. Neubauer, Revisiting Mednick's model on creativity-related differences in associative hierarchies. Evidence for a common path to uncommon thought. *J. Creat. Behav.* **47**, 273–289 (2013).

50. Q. Chen, R. E. Beaty, Z. Cui, J. Sun, H. He, K. Zhuang, Z. Ren, G. Liu, J. Qiu, Brain hemispheric involvement in visuospatial and verbal divergent thinking. *Neuroimage* **202**, 116065 (2019).

51. C. J. Wertz, M. O. Chohan, R. A. Flores, R. E. Jung, Neuroanatomy of creative achievement. *Neuroimage* **209**, 116487 (2020).

52. M. Benedek, E. Jauk, in K.C.R. Fox & K. Christoff (Eds.), *The Oxford Handbook of Spontaneous Thought: Mind-Wandering, Creativity, and Dreaming* (Oxford University Press, 2018), pp. 285–298.

53. K. Japardi, S. Bookheimer, K. Knudsen, D. G. Ghahremani, R. M. Bilder, Functional magnetic resonance imaging of divergent and convergent thinking in Big-C creativity. *Neuropsychologia* **118**, 59–67 (2018).

54. M. Benedek, in *The Cambridge Handbook of the Neuroscience of Creativity*, R. E. Jung, O. Vartanian, Eds. (Cambridge Univ. Press, ed. 1, 2018), pp. 180–194.

55. T. Asari, S. Konishi, K. Jimura, J. Chikazoe, N. Nakamura, Y. Miyashita, Right temporopolar activation associated with unique perception. *Neuroimage* **41**, 145–152 (2008).

56. L. Aziz-Zadeh, J. T. Kaplan, M. Iacoboni, "Aha!": The neural correlates of verbal insight solutions. *Hum. Brain Mapp.* **30**, 908–916 (2009).

57. A. Abraham, S. Beudt, D. V. M. Ott, D. Yves von Cramon, Creative cognition and the brain: Dissociations between frontal, parietal–temporal and basal ganglia groups. *Brain Res.* **1482**, 55–70 (2012).

58. E. G. Chrysikou, C. Jacial, D. B. Yaden, W. van Dam, S. B. Kaufman, C. J. Conklin, N. A. Wintering, R. E. Abraham, R. E. Jung, A. B. Newberg, Differences in brain activity patterns during creative idea generation between eminent and non-eminent thinkers. *Neuroimage* **220**, 117011 (2020).

59. B. Garcin, M. Urbanski, M. Thiebaut de Schotten, R. Levy, E. Volle, Anterior temporal lobe morphometry predicts categorization ability. *Front. Hum. Neurosci.* **12**, 36 (2018).

60. C. Aichelburg, M. Urbanski, M. Thiebaut de Schotten, F. Humbert, R. Levy, E. Volle, Morphometry of left frontal and temporal poles predicts analogical reasoning abilities. *Cereb. Cortex* **26**, 915–932 (2016).

61. B. Shi, X. Cao, Q. Chen, K. Zhuang, J. Qiu, Different brain structures associated with artistic and scientific creativity: A voxel-based morphometry study. *Sci. Rep.* **7**, 42911 (2017).

62. A. Abraham, B. Rutter, T. Bantin, C. Hermann, Creative conceptual expansion: A combined fMRI replication and extension study to examine individual differences in creativity. *Neuropsychologia* **118**, 29–39 (2018).

63. M. Jung-Beeman, Bilateral brain processes for comprehending natural language. *Trends Cogn. Sci.* **9**, 512–518 (2005).

64. C. Chiarello, N. A. Kacinik, C. Shears, S. R. Arambel, L. K. Halderman, C. S. Robinson, Exploring cerebral asymmetries for the verb generation task. *Neuropsychology* **20**, 88–104 (2006).

65. K. C. Aberg, K. C. Doell, S. Schwartz, The "Creative Right Brain" revisited: Individual creativity and associative priming in the right hemisphere relate to hemispheric asymmetries in reward brain function. *Cereb. Cortex* **27**, 4946–4959 (2017).

66. E. Jauk, A bio-psycho-behavioral model of creativity. *Curr. Opin. Behav. Sci.* **27**, 1–6 (2019).

67. Y. Kenett, S. L. Thompson-Schill, Novel conceptual combination can dynamically reconfigure semantic memory networks (2020); doi:10.31234/osf.io/crp47.

68. M. Karwowski, M. Czerwonka, E. Wiśniewska, B. Forthmann, How is intelligence test performance associated with creative achievement? A meta-analysis. *J. Intell.* **9**, 28 (2021).

69. T. Lubart, F. Zenasni, B. Barbot, Creative potential and its measurement. *Int. J. Talent Dev. Creat.* **1**, 41–50 (2013).

70. Y. N. Kenett, E. Levi, D. Anaki, M. Faust, The semantic distance task: Quantifying semantic distance with semantic network path length. *J. Exp. Psychol. Learn. Mem. Cogn.* **43**, 1470–1489 (2017).

71. M. E. J. Newman, Modularity and community structure in networks. *Proc. Natl. Acad. Sci. U.S.A.* **103**, 8577–8582 (2006).

72. M. Rubinov, O. Sporns, Weight-conserving characterization of complex functional brain networks. *Neuroimage* **56**, 2068–2079 (2011).

73. E. Jauk, M. Benedek, A. C. Neubauer, The road to creative achievement: A latent variable model of ability and personality predictors. *Eur. J. Pers.* **28**, 95–105 (2014).

74. P. Kundu, N. D. Brenowitz, V. Voon, Y. Worbe, P. E. Vértes, S. J. Inati, Z. S. Saad, P. A. Bandettini, E. T. Bullmore, Integrated strategy for improving functional connectivity mapping using multiecho fMRI. *Proc. Natl. Acad. Sci. U.S.A.* **110**, 16187–16192 (2013).

75. C. J. Lynch, J. D. Power, M. A. Scult, M. Dubin, F. M. Gunning, C. Liston, Rapid precision functional mapping of individuals using multi-echo fMRI. *Cell Rep.* **33**, 108540 (2020).

76. C. Gaser, R. Dahnke, CAT-A computational anatomy toolbox for the analysis of structural MRI data (2016); https://www.semanticscholar.org/paper/CAT-A-Computational-Anatomy-Toolbox-for-the-of-MRI-Gaser-Dahnke/2682c2c5f925da18f465952f1a5c904202ab2693.

77. A. Abraham, F. Pedregosa, M. Eickenberg, P. Gervais, A. Mueller, J. Kossaifi, A. Gramfort, B. Thirion, G. Varoquaux, Machine learning for neuroimaging with scikit-learn. *Front. Neuroinform.* **8**, 14 (2014).

78. J. D. Power, A. Mitra, T. O. Laumann, A. Z. Snyder, B. L. Schlaggar, S. E. Petersen, Methods to detect, characterize, and remove motion artifact in resting state fMRI. *Neuroimage* **84**, 320–341 (2014).

79. A. Fornito, A. Zalesky, M. Breakspear, Graph analysis of the human connectome: Promise, progress, and pitfalls. *Neuroimage* **80**, 426–444 (2013).

80. V. Latora, M. Marchiori, Efficient behavior of small-world networks. *Phys. Rev. Lett.* **87**, 198701 (2001).

81. M. Xia, J. Wang, Y. He, BrainNet Viewer: A network visualization tool for human brain connectomics. *PLOS ONE* **8**, e68910 (2013).

82. A. F. Hayes, *Introduction to Mediation, Moderation, and Conditional Process Analysis, Second Edition: A Regression-Based Approach* (Guilford Publications, 2017).